Photovoltaic System Design for DC House

A Senior Project

presented to the

Faculty of the Electrical Engineering Department

California Polytechnic State University, San Luis Obispo

In Partial Fulfillment

of the Requirements for the Degree

Bachelor of Science

by

Luis B. Perez
Hao Ming Mai

Sunday, June 05, 2011

Table of Contents

List of Tables and Figures

Table **Page**

Figures

Acknowledgements

The students would like thank the following for their contribution for our senior project:

- Professor Taufik for suggesting and providing the opportunity to design the Solar Photovoltaic System of his DC House Project as well as providing technical advice.
- Professor Ahlgren for technical advice and suggestions on solar panel orientation.
- Allan Soriano for technical advice and suggestions on designing the DC-DC converter and reviewing the report.
- John Bedoya for advice and suggestions on constructing the solar panel frame.
- National Semiconductor for donating three LM5088-1 Evaluation Boards.
- Coilcraft for donating a tray of ten high quality 15µH inductors.
- National Renewable Energy Laboratory for providing the System Advisor Model software to simulate solar panel output power.

Abstract

The objective of this project is to research and design a practical 200W photovoltaic system at the lowest cost and highest efficiency in order to support the DC House Project. The impetus for this project stems from the necessity of delivering energy to people in developing countries who otherwise lack the benefits of electricity. The Photovoltaic System Design is divided into two main parts, the buck DC-DC converter and the optimized photovoltaic panel. The converter consists of schematics, efficiency calculations, load/line regulation calculations, component comparisons, data plots from simulations and testing. The optimized photovoltaic panel section includes component comparisons, complete construction drawings, PV advantages, and array characteristics.

About the Authors:

Luis "Luigi" Perez and Hao Ming "Andrew" Mai are Cal Poly students studying Electrical Engineering with an emphasis in Power Systems. The students also have a strong interest in Power Electronics and Renewable Energy. When presented with the opportunity to contribute to the DC House Project, the students jumped at the chance to design the photovoltaic system portion of the overall project.

I. Introduction

According to recent studies, one-quarter of the world's population live without electricity. Without electricity there will be no clean water available, no safe medical care, and unhealthy food supplies. Many people living in developing countries often use wood, lumps of coal or even dung to heat and cook in their homes, resulting in indoor air pollution that roughly kills 1.6 million people a year [1]. Also, these countries lag in human development and further propagating poverty. These problems are caused by two main factors: location, where utility grid is out of reach or geographically inaccessibility, and poverty.

First of all, transmission lines are relatively expensive, requiring constant monitoring and maintenance. Therefore, in the utility companies' perspective, having transmission lines traverse across forests, bodies of water or over mountains to supply electricity to a small town or village is not cost effective. Although some countries have supplied electricity to rural areas, delivery is highly unreliable. For example, when the load on the entire power system exceeds available capacity, rural areas are cut first, frustrating customers who subsequently refuse to pay their electricity bill for services not rendered. Furthermore, many people who are unable to afford electricity steal from the grid by tapping onto energized transmission lines. Such unauthorized tapping disrupts the whole grid with unplanned loads drawing power from the system, as well as the extreme danger tapping onto “hot” lines by undereducated and untrained people.

One way to distribute electricity from the grid is by using the Single Wire Earth Return (SWER) method which transmits through a single phase line and then using the earth or

some body of water as a return path instead of another transmission line. The advantage of the SWER method is safety; the transformer isolates the ground from the source (grid) [2].

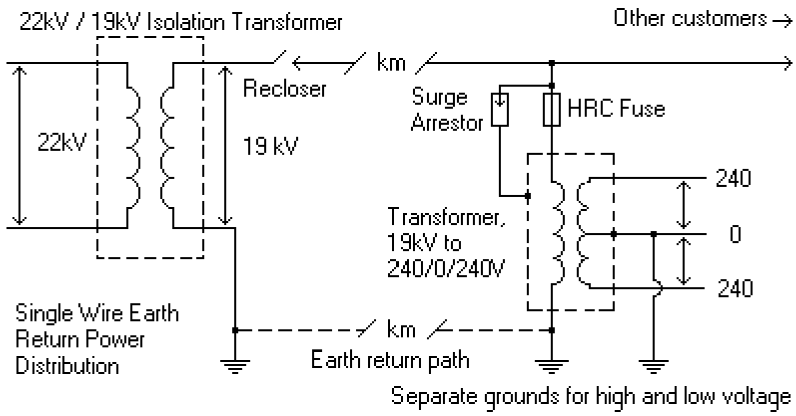

Figure 1-1. Single Wire Earth Return Circuit Providing 240V to the Customer [2]

This method is relatively low cost since it uses one conductor instead of several conductors, and is reliable since it has fewer components thus reducing the probability of failure. The disadvantage of this system is that once a fault occurs, the connected load will be lost. Also, the method is not very efficient due to the long-distance line losses, resulting in poor regulation. Also of concern is the low power factor due to the high reactance of the single line. Many countries use this method but other countries have deemed it unsuitable.

Renewable resources such as the sun can provide an alternative energy source to people in remote areas of developing countries, where expanding the traditional electrical grid becomes economically inefficient. Solar panels are known for capability of turning solar energy into electricity. Solar panels do not produce any local pollution, does not require fuel consumption, possesses size flexibility, simple maintainability since no moving parts, and produces no noise. Some disadvantages for solar panels are the prohibitively high

cost, dependency on climate variability, and does not provide continuous energy throughout the day [3].

Wind power uses the location's winds to produce energy. Wind turbines are mainly used in the wind power systems. Some advantages of wind turbines is that they take small plot of land, are built in different sizes, don't need any other type of consumptions, does not produce any pollution, and are renewable as long as there is wind around there to keep them producing electricity. Some disadvantages for wind turbines is that they are prone to damage in bad weathers, some may hurt animals with the blades, can be very noisy, and depend the strength of the wind in the location installed in [4].

Hydropower systems, such as small dams, have the ability to use water currents to drive their turbines into making electricity. Small dams have the advantage to be design for inexpensive repairs and maintenance. One can control the electricity easily shutting down if necessary. Dams can produce constant energy for years and does pollute the environment. Some disadvantages from dams are the potential to cause floods to nearby communities, cause ecosystems to be destroyed, take relatively longer and could be expensive to build [5].

These are other ways to provide electricity to areas that lack electricity but all of them contain advantages and disadvantages. For the DC project house, which would provide a house with accessible and reliable electricity for people in this situation, it will obtain its energy from different resources: solar, wind, hydropower, and even including human energy. The project will consist of different phases, with the first being the DC house modeling and the electrical systems from the different resources. With greenhouse gas

emissions escalating every year, using renewable resources in the prototype of the DC house will be avoid producing greenhouse gases and promote the use of renewable resources. The resources will not only be portable but also efficient since with the energy sources a DC to DC converter will be implemented, having the advantage of being more efficient than a DC to AC converter.

The prototype that this project partakes will not only be flexible but will adjust to the max cost efficient according to the environment and location of the remote places that need electricity. For example, if the location does not have a river or stream but has fairly strong winds and an abundance of daylight, then the system implemented in that location will concentrate more on both wind power and solar power. The DC House project will have the ability for each location to use whatever they have their advantage to.

II. Background

Throughout history, solar cells and panels have been expensive, up to $300/Watt. As the solar cells became part of satellites, it has merged itself into other industries including railway companies. Cost of solar panel began dropping and that was how it started going into the public industry. Not only has cost decreased but also the increase of its efficiency by up to 42% efficiency for solar cells that had made their use to become more prevalent [6]. According to European Photovoltaic Industry Association, the price of solar panel dropped from $3.7/Watt in 2007 to $1.8/Watt in 2010. With the decrease in price, a global solar installation of 182GWatt in 2010, this is a growth of 139% over 2009 [7].

Although the growth of photovoltaic (PV) systems significantly increased over the years, the efficiency of the panels is still one of the main factors. Therefore, finding other ways to optimize the solar panel is also a key to improve the efficiency of the photovoltaic system since the solar panels that are being used in this project have an efficiency of 13%. One characteristic of the solar panel is that as it receives solar arrays it will heat up. Heating up the solar panel will actually decrease its efficiency. Finding ways to decrease the heating problem of the solar panel will help it maintain its efficiency throughout its recollection of energy from the sun.

In conjunction with PV panels are the converters. Converters, which came in about the late 70's, have been useful throughout industry. There are widely used in even at personal level, for example, power adapters of laptops, cell phones, battery chargers, etc. Converters vary from DC-to-AC to DC-DC and a derivation of that. For PV applications,

the most commonly used converters are inverters and DC-DC converters. Inverters are used to convert DC electricity from sources such as batteries, fuel cells, and as well as solar panels to AC electricity. Converter is an electronic circuit that converts a voltage from a source to voltage level to another, which includes AC-to-AC converter and DC-DC converter. A DC-DC converter in the project will be examined to provide good efficiency since it will minimize the power loss in the system and any other cost if the converter was DC-to-AC. Implementing efficient components in the converter will allow it to come into specification with the project.

III. Requirements

In the photovoltaic system, optimizing the solar panel and implementing a well efficient DC-DC converter is required. Finding a way to increase the efficiency and maintain a reasonable efficiency of the solar panel should be done. Data should be taken from the solar panel throughout the day. A multimeter will be used to measure the open circuit current and the open circuit voltage as accurate as it could be done. This should be done before and after the optimization. The peak measurements of the solar panel should be found in order to design the DC-DC converter. All these measurements will be conducted in a suitable location where plentiful of sunlight amount could be captured by the solar panel.

The DC-DC converter should be able to handle the voltage and current from the solar panel. The converter should output a voltage 24V and output current of about 8.3A. Since this system will be about 200W, a cooling system or a heat sink may be implemented with the converter. Also, connections will be implemented in the converter since it is going to be connected to the solar panel and to other components leading to the DC house. Finding the right components of the converter should be done without overspending and also acquiring backup components in case some components fail. Simulations of the converter will be done before soldering the components into the board. A demonstration board will be made with all the components soldered either through-hole or surface mount, depending on the components that are going to be used. Testing will be done in the Power Electronics Lab. The converter will be tested with the solar panel connected to it. This will help verify all the specifications and find any discrepancies within the project.

IV. Design

The goal of this project was to design a photovoltaic system that converts at least 90% of a 200W solar panel into an output voltage of 24V at 8.3A. With the change in seasons, the solar panel can be manually adjusted to tilt at an optimum angle that maximizes the panel's average output power. The solar panel has three different settings for the four different seasons: summer (7°), autumn/spring (32°), and winter (55°). Each setting would be designed in accordance to the latitude of its location. Once the solar panel is adjusted to its optimal angle, the companion mirror will correspondingly be adjusted to direct more sunlight to the solar cells; the mirror is half the area of the solar panel, placed facing the panel, and on its own supports.

Once the solar panel is set to its optimal settings, the DC-DC converter was designed to take a range of input voltages from a high of 40V to low of 26.41V and down converted to the required 24V output voltage. Throughout a typical sunny day, the input voltage should remain above than the dropout voltage (minimum input voltage), thereby keeping the DC-DC converter working properly and maintaining a regulated 24V output voltage.

There are multitudes of semiconductor vendors offering a variety of solutions to down convert from a 200W solar panel to an output voltage of 24V. Since this project is intended to be incorporated into the DC House Project for developing societies, cost and efficiency are paramount in developing this system. After researching costs, simplicity, and performance from a variety of analog semiconductor companies, the LM5088 from National Semiconductor was selected as the project's buck converter.

A. Synchronous versus Non-synchronous

Choosing the right DC-DC converter to meet the requirements took several steps. First, we had to decide if we wanted a synchronous or non-synchronous converter. A synchronous buck converter has two power MOSFETs alternately turning on and off 180° out of phase from each other. A non-synchronous buck converter uses one power MOSFET high-side and a power Schottky diode on the low-side. One of the main advantages of synchronous converters is that the voltage drop across the low-side MOSFET $R_{(DS)ON}$ can be lower than the voltage drop across a power diode of the non-synchronous converter. Thus, the synchronous converter may have lower power dissipation loss, hence increasing the efficiency. Non-synchronous converters operate with a power diode instead of a bottom gate MOSFET resulting in only one MOSFET switching as opposed to the synchronous converter with two power MOSFETs under control. The more complex synchronous converter relies on a controller ensuring the top and bottom gate do not turn on simultaneously and provides the drive to turn both power MOSFETs on when required. If both MOSFETs were turned on simultaneously a "shoot through" current (a short circuit) could severely damage the circuit since the source and ground will be directly connected. Cross conduction would overload and damage parts, if not all, the converter [8].

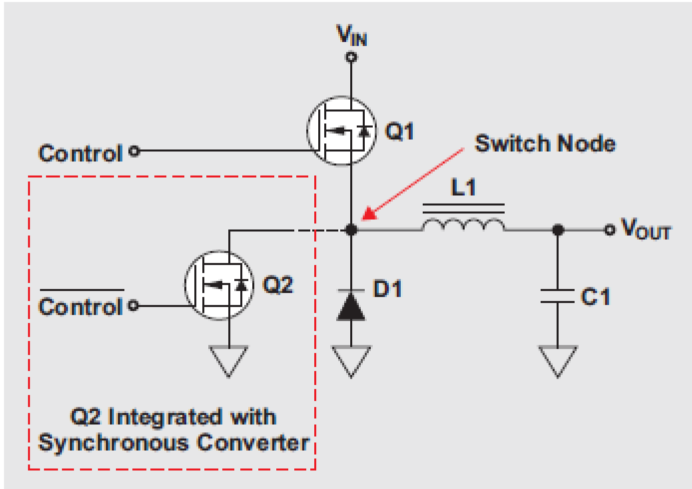

Figure 4-1. Synchronous and non-synchronous buck converter topology [8]

The question of synchronous versus non-synchronous efficiency for buck regulators was tested and studied by Texas Instruments. Tests showed that at lower output voltages, synchronous buck converters are generally more efficient than non-synchronous buck converters [8]. In the non-synchronous topology, the Schottky diode conducts more often than the charging MOSFET (top gate) with low output voltages. The forward voltage (V_F) drop across the diode contributes significantly to power loss ($V_F * I$) during (1- D) conduction. Testing showed that when the output voltage was increased from 1.5V to 2.5V, the results yielded comparable efficiencies between synchronous and non-synchronous architectures. In this case, the power diode in the non-synchronous converter conducted less often than the top gate power MOSFET, meaning fewer losses in the system. Another interesting conclusion was that with light loads, non-synchronous converters were running in discontinuous mode. The decrease in DCR parasitic loss is attributed to the current flowing in one direction as oppose to the continuous mode of the synchronous converter, where current travels in either the top gate or the bottom gate. Since we are dealing with high output and high loads, having a

non-synchronous buck converter would be as efficient as a synchronous buck converter. Nevertheless, the non-synchronous buck converter would only have to worry about controlling the switching of one power MOSFET, making it more reliable and reducing the probability of not functioning [8].

Using National Semiconductor's power supply design website, WEBENCH®, we compared different types of design that could accomplish the specifications of the project. As explained before, both synchronous and non-synchronous are going to be efficient enough to be operating in the project since it will output 200W.

Part	Create	WEBENCH Tools	Schematic	BOM Images	Design Considerations	LDO	Temp (deg)	BOM Footprint (mm2)	BOM Cost	Eff (%)	BOM Count	Freq (kHz)	Vout p-p (mV)
LM3150	Open Design			1534mm²	SIMPLE SWITCHER(r) Controller	N	84.36	1534	$13.44	98%	20	179	617.25
LM25119	Open Design			3064mm²	42V Interleaved Output Synchronous Buck Controller	N	90.81	3064	$9.19	98%	35	248	138.66
LM5119	Open Design			3064mm²	65V Dual Output Synchronous Buck Controller	N	90.81	3064	$9.44	98%	35	248	138.66
LM25088	Open Design			798mm²	42V BUCK CONTROLLER	N	50.94	798	NA	98%	34	186	192.02
LM5088	Open Design			798mm²	75V Buck Controller	N	50.94	798	NA	98%	34	186	192.02

Figure 4-2. WEBENCH® comparison of various types of buck converters from National Semiconductor [9]

As we can see from the above figure, we see many similarities between the various buck regulators but the LM5088 operates at higher efficiency without as much heat loss. The LM5088 also has a low peak-to-peak output ripple voltage. Nonetheless, the circuit is

relatively simple to assemble and compact in size. Consequently, LM5088 synchronous DC-DC converter was chosen as the base for our photovoltaic system design [9].

B. Setting the Oscillator Frequency

The oscillator's frequency of the converter can be adjusted by changing the resistance R_{RT}:

$$R_{RT} = \frac{\frac{1}{fsw} - 280ns}{152pF} \quad (4\text{-}1)$$

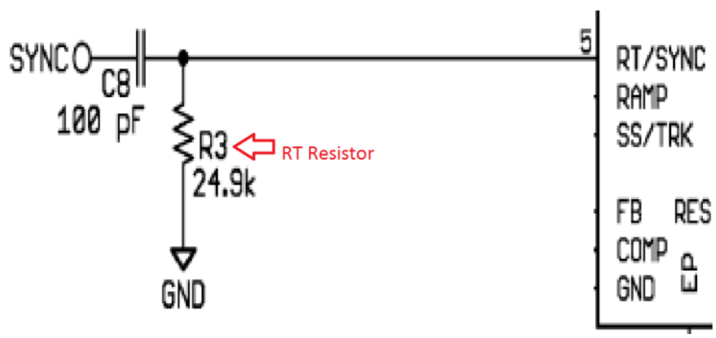

Figure 4-3. Location of Where RT Resistor is Place with the Converter.

The frequency that was wanted for the design was 250kHz, therefore, using equation 4-1, the resistor that would be place between pin 5 and ground is [10]:

$$R_{RT} = \frac{\frac{1}{250kHz} - 280ns}{152pF} = \ 24{,}473\Omega$$

The resistor that was the closest to the value calculated above was 24. 9k**Ω** and was used as the R_{RT}.

C. Dropout Voltage Reduction

Dropout voltage is the difference between the minimum input voltage to maintain regulation and the output voltage. Equation 4-2 determines at which low voltage the converter will maintain regulation.

$$Dropout\ Voltage = V_{out}\ x\ \frac{T_{off(max)}}{T_{OSC} - T_{off(max)}} \qquad (4\text{-}2)$$

$$\frac{T_{OFF\ (\max)}}{T_{OSC} - T_{OFF(\max)}} = the\ maximum\ duty\ cycle$$

$T_{OSC} = 1/f_{SW}$

T_{OFF} = forced off-time

The minimum voltage to maintain regulation is:

$$Dropout\ Voltage = V_{OUT}\ x\ \frac{T_{OFF\ (\max)}}{T_{OSC} - T_{OFF(\max)}} = 24\ x\ \frac{365ns}{4\mu s - 365ns} = 2.41V$$

$$V_{IN\ min} = V_{OUT} + dropout\ voltage = 24 + 2.41 = 26.41V$$

According to the calculation, since we want to output a voltage of 24V, our input to the converter cannot be lower than 26.41V.

One can manipulate the switching frequency by changing the oscillator's frequency, which is done by changing the RT resistor. By doing so, one can change the dropout voltage [10].

D. Choosing Output Inductor

From the LM5088 datasheet, the output current ripple is preferred to be 20% to 40% of the output load. Equation 4-3 helps calculate what inductor value would be proper for certain requirements.

$$L = \frac{V_{out}}{I_{PP} x\, f_{sw}} x \left(1 - \frac{V_{out}}{V_{in(max)}}\right) \quad (4\text{-}3)$$

For I_{pp} being 40% of I_{out}:

$$L = \frac{24V}{(8x0.40) x\ 250kHz} x \left(1 - \frac{24}{36}\right) = 10\mu H$$

For I_{pp} being 20%:

$$L = \frac{24V}{(8x0.20) x\ 250kHz} x \left(1 - \frac{24}{36}\right) = 20\mu H$$

To prevent saturation the inductor should be rated to the highest peak of the current. We had an inductor with a value of 15µH. Since this falls in the recommended range, we decided to implement it to the circuit board. The resulting Ipp from the chosen inductor is:

$$I_{PP} = \frac{V_{OUT}}{Lxf_{sw}} x \left(1 - \frac{V_{out}}{V_{in(max)}}\right) = \frac{24V}{15\mu Hx250kHz} x \left(1 - \frac{24V}{36V}\right) = 2.1A$$

The inductor that was chosen had an I_{sat} of about 18A. Also, we ordered a sample from Coilcraft, and they sent us inductors with 1% tolerance which would make the converter to be more accurate. The inductor's DCR was 2.6mΩ, relatively higher than the other

inductors in the series, but a very low DCR when compared to other inductors in the market [10].

E. Output Voltage Divider

R_{FB1} and R_{FB2} could be adjusted to set a desire output voltage. Since we are aiming to have an output voltage of 24V, we decided to change R_{FB1} and keep R_{FB2} constant. Equation 4-4 shows the relationship between the output voltage and the feedback resistors [10].

$$\frac{R_{FB2}}{R_{FB1}} = \frac{V_{out}}{1.\ 205\ V} - 1 \qquad (4\text{-}4)$$

$$\frac{R_{FB2}}{R_{FB1}} = \frac{V_{out}}{1.205\ V} - 1 = \frac{24V}{1.205V} - 1 = 18.92$$

$$R_{FB1} = \frac{R_{FB2}}{18.92} = \frac{5.11k\Omega}{18.92} = 270\Omega$$

F. Current Sense Resistor

The original current sense resistor was 10mΩ and it was limiting the current through the inductor. The output current would reach currents up to 4A. When the current sense resistor was switched to 7mΩ, the output current of the converter was able to reach 8A. This amperage was one of the goals of the project since it would be able to provide 200W output [10]. Equation 4-5 calculates the necessary R_S to meet the requirements of the design:

$$R_S = \frac{V_{CS}/_A}{(1+margin)x\,(I_{out}+0.\;5xI_{PP})+\frac{V_{out}}{L\,x\,f_{SW}}} \qquad (4\text{-}5)$$

With the following parameters:

A=10V/V Vcs = 1.2V

I_{out} = 8A I_{pp} = 40% x 8 A = 3.2A

Margin = 0.1 V_{out} = 24V

$$R_S = \frac{1.2/_{10}}{(1+0.1)x\,(8+0.\;5x3.2)+\frac{24}{15\mu H\;x\;250kHz}} = 7.5m\Omega$$

G. Ramp Capacitor

This capacitor is necessary for the emulation ramp circuit in the IC [10]. The ramp capacitor suitable for our converter was calculated by the equation 4-6.

$$C_{RAMP} = \frac{g_m x\;L}{A\;x\;R_s} \qquad (4\text{-}6)$$

$$C_{RAMP} = \frac{g_m x\;L}{A\;x\;R_s} = \frac{5\frac{\mu A}{V}\,x\;15\mu H}{10\frac{v}{v}\,x7.6m\Omega} = 987pF$$

Capacitor of 1nF was selected as the ramp capacitor.

H. Cycle-by-Cycle Current Limit

The cycle-by-cycle current limit is set to decide the highest allowable current through the circuit. This protects the FET from the effects of saturation of the inductor. I_{peak}, in equation 4-7, is the highest current allowed to flow through the converter [10].

$$I_{peak} = \frac{1.2V - 25\mu A\ x\ \frac{V_{out}}{V_{in} x f_{SW} x C_{RAMP}}}{A\ x\ R_S} \tag{4-7}$$

A = 10V/V as the current sense amplifier gain from the datasheet.

C_{RAMP}= Ramp capacitor

R_S = sense resistor

$$I_{peak} = \frac{1.2V - 25\mu A\ x\ \frac{V_{out}}{V_{in} x f_{SW} x C_{RAMP}}}{A\ x\ R_S} = \frac{1.2V - 25\mu A\ x\ \frac{24V}{36V x\ 250\ kHz\ x\ 987pF}}{10\ v/v\ x\ 7.6m\Omega}$$

I_{peak} = 15A

This means that the maximum output current could be up to 15A but not necessarily be that output.

I. Bypass Capacitor

One of the components that the converter is utilizing is a bypass capacitor also called decoupling capacitors. Decoupling capacitors are used to reduce unwanted AC signals riding on DC supply circuits. Bypass capacitor eliminates voltage droops on the power supply by storing electric charge to be released when a voltage spike occurs. Having the

bypass capacitor directly connected to the power supply would enhance its effectiveness by having a high self-resonant frequency or useful bandwidth. This is because no additional series inductance would be on the path between the capacitor and the power supply. A capacitor of 1µF is placed in between the ground and Vcc. This capacitor is also placed between the input voltage and the ground. The capacitor prevents deregulation when the voltage is dropping [11].

J. Output Capacitor

The output capacitor smoothes the inductor output current ripple. Finding the correct value for the output capacitor depends on the parameters of the converter. One of the main parameters is the inductor and the output current ripple. Using equation 4-8, we can calculate the necessary output capacitor for the converter [10].

$$C_O = \frac{L\ x\left(I_O + \frac{\Delta I_{PP}}{2}\right)^2}{(\Delta V + V_{OUT})^2 - {V_{OUT}}^2} \qquad (4\text{-}8)$$

$$C_O = \frac{L\ x\ \left(I_O + \frac{\Delta I_{PP}}{2}\right)^2}{(\Delta V +\ V_{OUT})^2 - {V_{OUT}}^2} = C_O = \frac{15\mu H\ x\ \left(8A + \frac{2A}{2}\right)^2}{(240mV +\ 24V)^2 - 24V^2} = 112\mu F$$

The chosen output capacitor value was around 112 µF. This capacitor should maintain an output voltage ripple maximum of 240mV.

K. Solar Panel Design

Currently, there are four main types of solar panels that are commercially available: monocrystalline silicon panel, polycrystalline silicon panel, string ribbon silicon panel, and amorphous silicon panel. Since the amorphous silicon panel is composed of a piece of semi conductive material, like copper, with a thin silicon film over the top that is attached to some metal pieces, it has the lowest efficiency, from 5 to 6%. Although this type of panel is very cheap, it will not be cost effective in the long run.

On the other hand, monocrystalline silicon panels are made from single silicon crystals. Therefore, the panels have the highest efficiency out of the four at 14 to 18%. However, since it takes longer to manufacture larger silicon crystals, monocrystalline silicon panels are the most expensive. Polycrystalline silicon panels are made up of several individual PV cells that have metal conducting materials and have efficiencies of 12 to 14%. Moreover, string ribbon silicon panels are made in a similar fashion as polycrystalline silicon panels with solar cells made with strips of silicon. Out of the four types of panels, polycrystalline silicon panels are the cheapest to manufacture, with the savings passed on to the consumers [12]. Also, the efficiency of these panels is high compared to amorphous silicon panels and just slightly lower than that of monocrystalline silicon panels. Furthermore, another advantage of polycrystalline silicon panels is lower maintenance as compared with monocrystalline, since damaging one of the cells does not require replacing the entire panel. Thus, due to low cost, high efficiency, and convenience, the polycrystalline silicon panel was chosen for this project.

Since the efficiency of commercially available solar panels is relatively low, such as the 13% efficiency panel being used for this project, maintaining the panel at its maximum potential is critical. The efficiency of the solar panel is mainly affected by two main criteria: the amount of the sunlight being received and the temperature of the panel.

The I-V characteristic of a solar cell is the same as that of a diode when light is shined onto it. However, when the cell is illuminated, the IV curve shifts downward and starts to generate power. As the intensity of the light being shined onto the cell increases, the I-V curve shifts as well. This is shown in Figure 4-4 with the shaded area denoting the amount of power generated. However, since the cell is generating power, the standard diode graph convention is inverted, as shown in Figure 4-5.

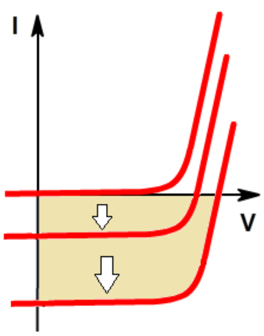

Figure 4-4. I-V Characteristic of a Solar Cell as Light Intensity Increases [13]

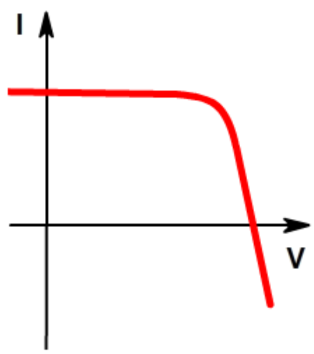

Figure 4-5. I-V Characteristic Convention of a Solar Cell [13]

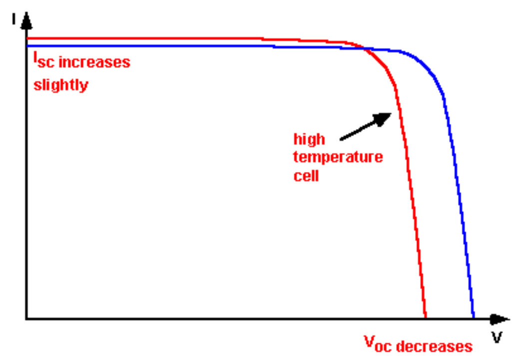

Figure 4-6. I-V Characteristic of a Solar Cell with Respect to Change in Temperature [13]

Like all other semiconductor devices, solar cells are sensitive to temperature, as shown in Figure 4-6. For the selected panel, there is an expected 0.42%/°C decrease in efficiency. Therefore, the main focus of this project is based on providing the solar panel with maximum sunlight, decreasing the solar cell temperature, and increasing the solar radiation intensity.

L. Solar Panel Cooling Methods

There are various ways to lower the solar panel temperature: cooling fans, liquid cooling, and traditional air convection. Cooling the solar cells with electric fans and liquid cooling system are extremely effective, however, for our purposes, these are inefficient power drains. Therefore, the traditional air convection method was selected for two main reasons. First, by elevating the panel by rotating it at the mounting surface allows adequate air-flow across the panel surface and decreases its overall temperature. Also, this traditional air convection method will decrease the cost and required maintenance of the system. Therefore, the solar panel will be implemented with a wooden stand that accomplishes these goals.

M. Orientation and Position of the Panel

The other important factor in solar panel efficiency optimization is maximizing the amount of sunlight harvested. The more sunlight absorbed by the solar cell, the higher the output power. In order to achieve this requirement, the orientation of the solar panel is critical. The popular method of using a solar tracking device to monitor the position of the sun and adjust the panel accordingly was observed. This method however, is expensive and due to its added circuitry, motors and power usage, it seemed a contradictory fit for enhancing efficiency. As a result, this implementation decreases the system's overall efficiency as well as increasing the cost of the system. Therefore, instead of implementing this system, the method of tilting the panel at fixed angles was selected.

Before deciding on what angles to select, an understanding of the earth-sun geometry was required. The earth orbits around the sun in an oval shape however it is not responsible for the change in seasons on earth. The orbit of the earth varies the amount solar radiation by roughly 6%. The change in seasons is actually caused by a 23.5° earth tilt angle with respect to the ecliptic, which is shown in Figure 4-7. Therefore, the panel's tilted angle should vary based on the season and location of the presented systems.

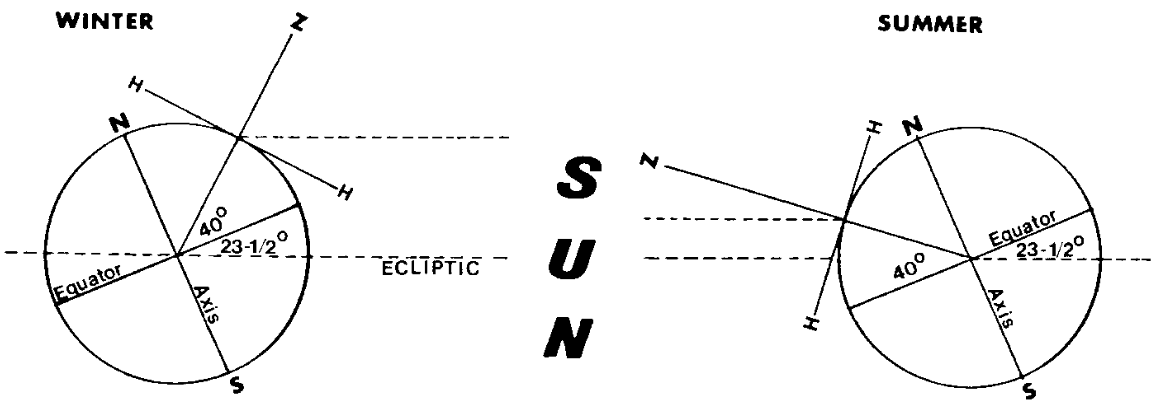

Figure 4-7. Angular Position or Tilt-Angle of Earth in Summer and Winter [14].

From MACS Laboratory Incorporated, the tilt angle of the panel can be calculated to optimize the amount of harvested sunlight in every season with the panel facing true south for the northern hemisphere, and true north for southern hemisphere. Since the winter season has the least sunlight exposure, the angle can be calculated by taking the latitude measurement of the panel location, multiplying it by 0.89, then added by 24°. For summer, the optimum angle will be the latitude measurement multiplied by 0.92, then subtracted by 24.3°. In addition, the optimum angle for spring and autumn is latitude multiplied by 0.98 then subtracted by 2.3° [15]. For example, the latitude of San Luis

Obispo, California is roughly 35°. Therefore, calculated optimum angles for this city will be as shown in Table 4-1 below.

TABLE 4-1
Optimum Panel Angles Throughout the Year

Seasons	Optimum Angles
Winter	7°
Summer	32°
Spring/Autumn	55°

N. Simulated Optimum Angle Results

By using professional software called System Advisor Model (SAM) from the National Renewable Energy Laboratory (NREL), each month's energy output was simulated with each solar panel angle displacement [16]. From the data shown in Table 4-2, the highlighted energy output is greater than the other two, which shows an increase in energy output due to different solar panel orientations. As compared to the recommended fixed angle of 35° throughout the year, which outputs an average of 34kWh, the multiple optimum angle arrangement increased this average to 35.4kWh. The 4.1% increase in energy output (Figure 4-8) seems insignificant in a single 200W panel; however, this output rise will be a viable quantity as the number of panels increases.

TABLE 4-2
Simulated Energy Output

	Monthly Enerygy Ouput With Panel Facing True South (kWh)			
	Summer	Spring/Autumn	Winter	
Month	7°	32°	55°	Combined
Jan	19.09	26.58	29.36	29.36
Feb	21.99	27.69	28.97	28.97
Mar	30.61	34.14	32.87	34.14
Apr	36.92	37.46	33.34	37.46
May	43.3	40.48	32.72	40.48
Jun	40.72	37.06	28.91	40.72
Jul	43.36	40.36	32.16	43.36
Aug	40.6	40.32	34.69	40.6
Sep	32.88	35.68	33.54	35.68
Oct	27.16	32.98	33.74	32.98
Nov	20.38	28.08	30.79	28.08
Dec	19.24	28.51	32.44	32.44

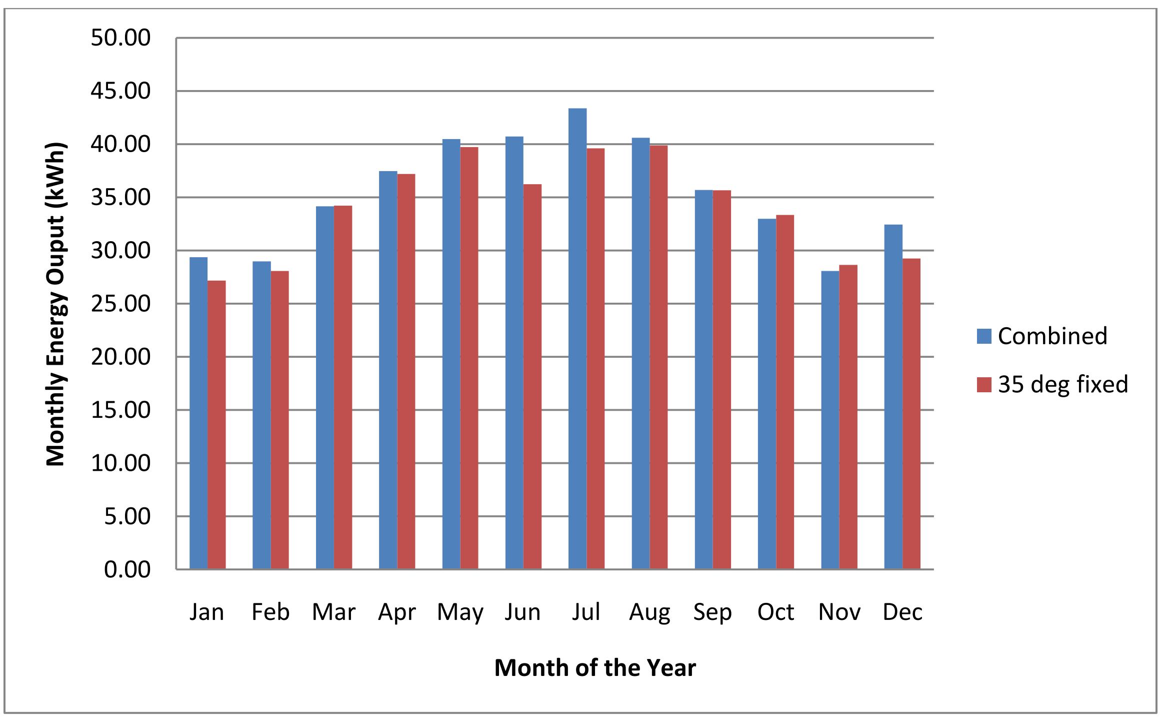

Figure 4-8. Comparison between new combined angles and 35° fixed angle

V. Test Plans

Prior to testing the complete photovoltaic system, individual components will be tested to compare with the data sheet. First, an open and short circuit test will be performed on the solar panel to measure the open circuit voltage and short circuit current. Also, the panel will be tested under loaded conditions to obtain the optimum operating voltage and current. Voltages and currents will also be measured with the solar panel and reflective mirror set at three angles corresponding to Summer (7°), Autumn/Spring (32°), and Winter (55°). The averaged data will be compared to the solar panel datasheet and simulated output power of the solar panel.

The DC-DC converter plays a vital role in this project and needed to be tested thoroughly. An unmodified National Semiconductor LM5088 buck converter evaluation board was tested to verify voltage and current compliance to the datasheet: input range of 5.5V to 55V, output voltage of 5V, maximum load current of 7A, and load regulation of less than 2%. After confirming the specifications were met, the buck regulator was modified to fit the project's electrical requirements. The input voltage ranged from the dropout voltage of 26.41V to as high as 55V, and the voltage measured 24.04V at 8.3A with a maximum load regulation of 2%. Lastly, the operating temperature of the converter was measured to determine if a heat sink was necessary.

After the solar panel and DC-DC converter were tested separately, they were then tested connected together. The results were similar to each components' individual measurement. All tests were conducted with a multimeter, an electronic load, a power supply, and an oscilloscope.

VI. Development and Construction

Adjustable Solar Panel Frame

In order for the panel to be tiltled at different optimum angles throughout the year, an adjustable frame is built. To keep the design simple and at a low cost, two triangular frames are built by wood to support the solar panel. Since traditional air convection cooling method is used, the frame will allow air to flow through easily.

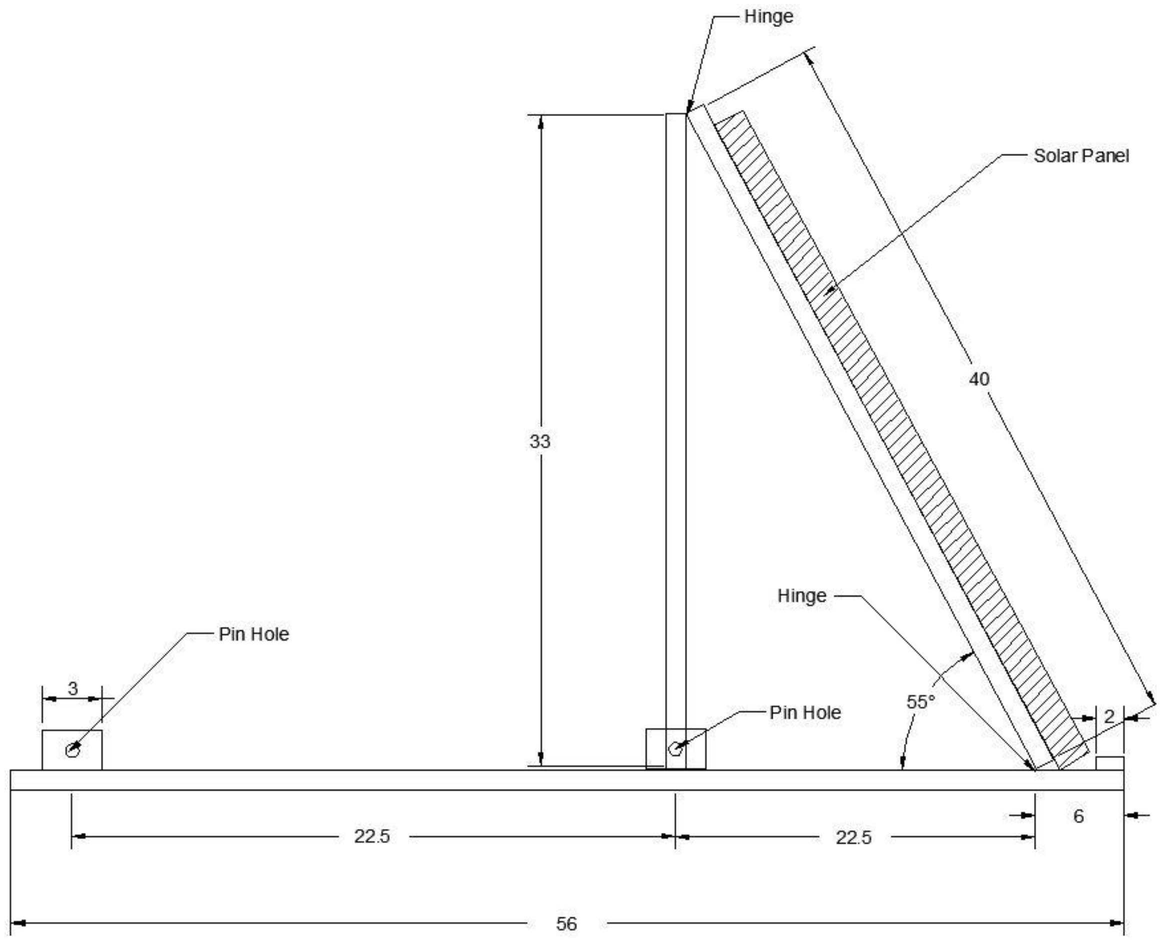

Figure 6-1. Side View of Solar Panel Adjustable Frame at 55°, units in inch

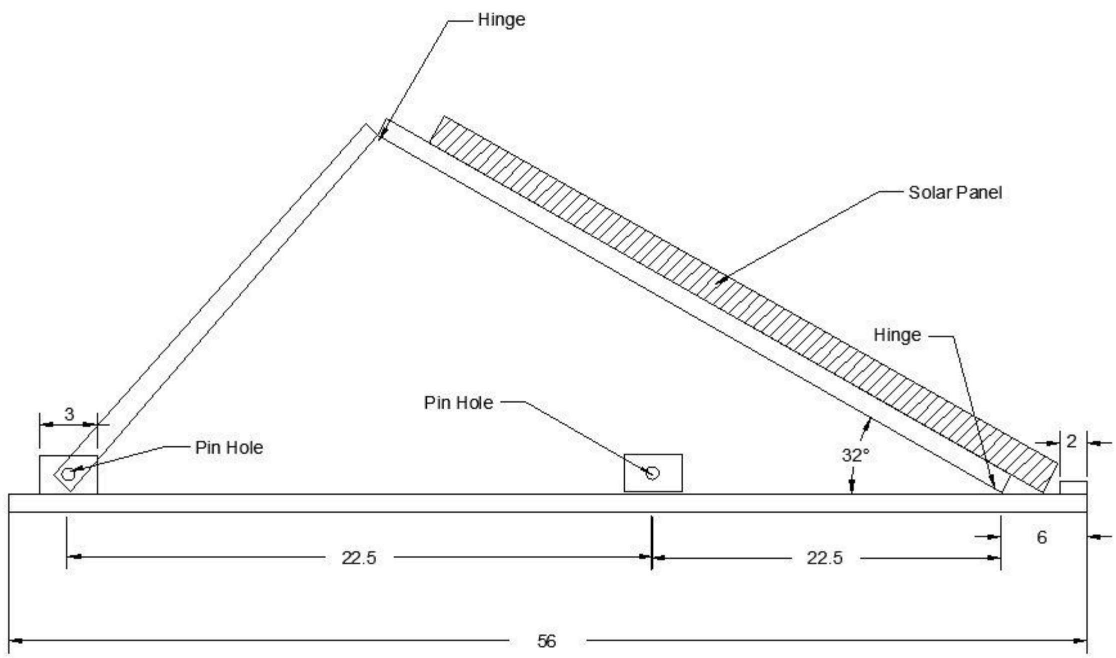

Figure 6-2. Side View of Solar Panel Adjustable Frame at 32°, units in inch

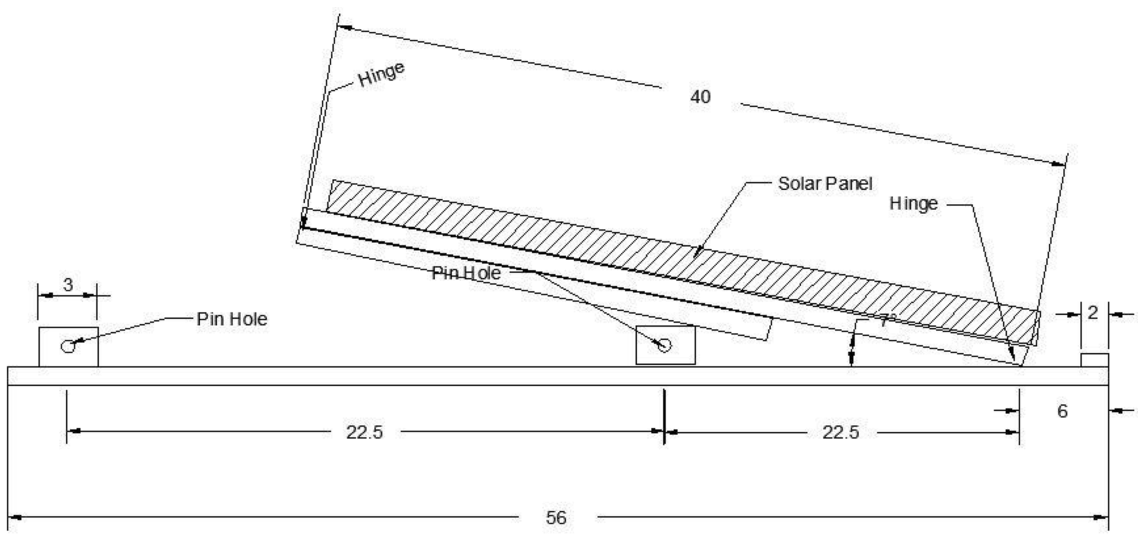

Figure 6-3. Side View of Solar Panel Adjustable Frame at 7°, units in inch

By using the geometry of triangles, dimensions of the frame is calculated. By following the design drawings, the two triangular frames are built, as shown from Figure 6-4 to Figure 6-6.

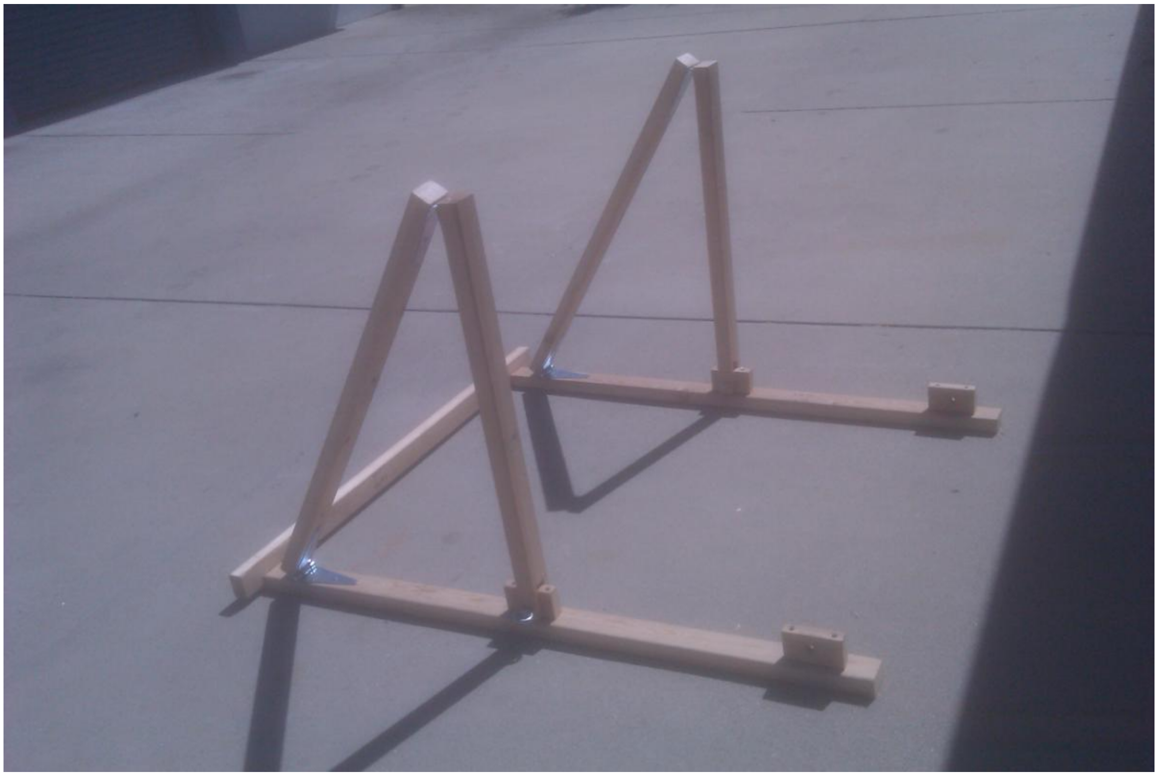
Figure 6-4. Adjustable Solar Panel Frame at 55°

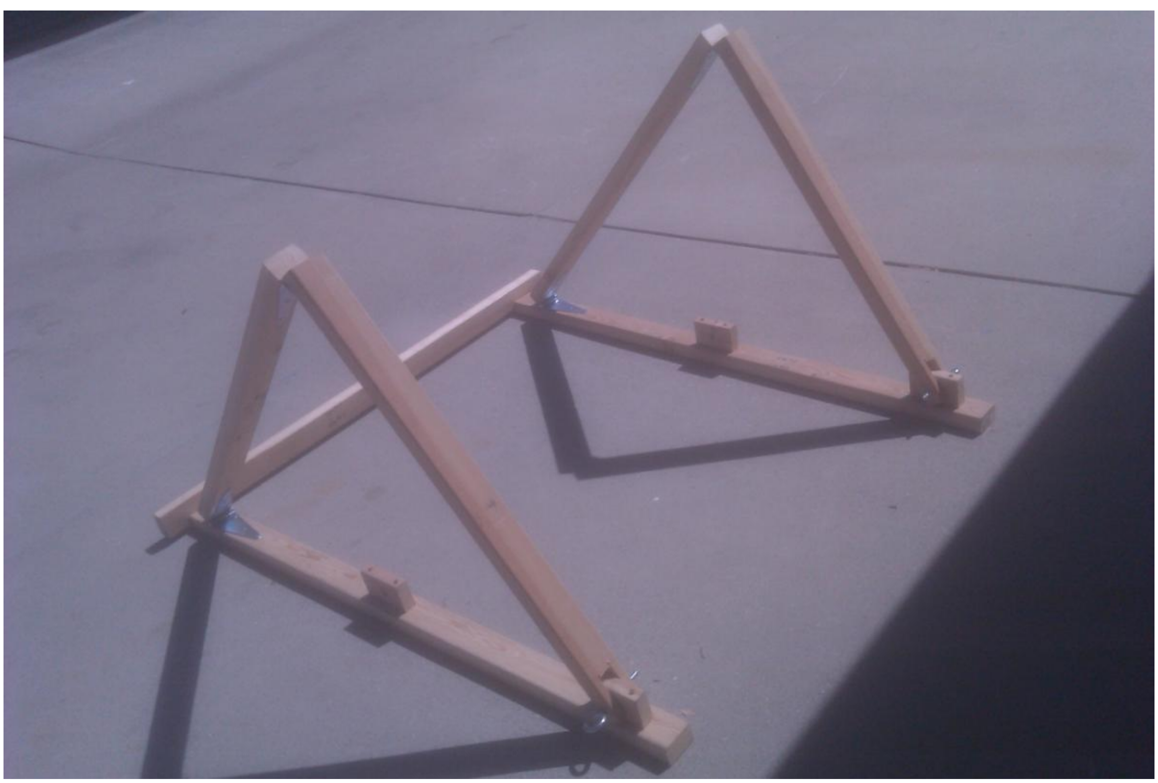
Figure 6-5. Adjustable Solar Panel Frame at 32°

Figure 6-6. Adjustable Solar Panel Frame at 7°

Figure 6-7. Solar Panel Tilted via Stand at 55°.

Figure 6-8 Solar Panel Tilted via Stand at 32°.

Figure 6-9. Solar Panel Tilted via Stand at 7°.

The method used for increased light intensity was done by implementing the solar panel with a reflecting mirror.   The tilted angles of the reflecting mirror were determined experimentally. Each of the solar panel's tilted angles was tested with various tilted reflecting mirror angles. After averaging all the data that was collected, the angles of the reflecting mirror frames, 37.5° and 53°, were determined. Since the width of the

reflecting mirror is 24 in.; the frames were designed according to that. Then two triangular frames for the reflecting mirror were built.

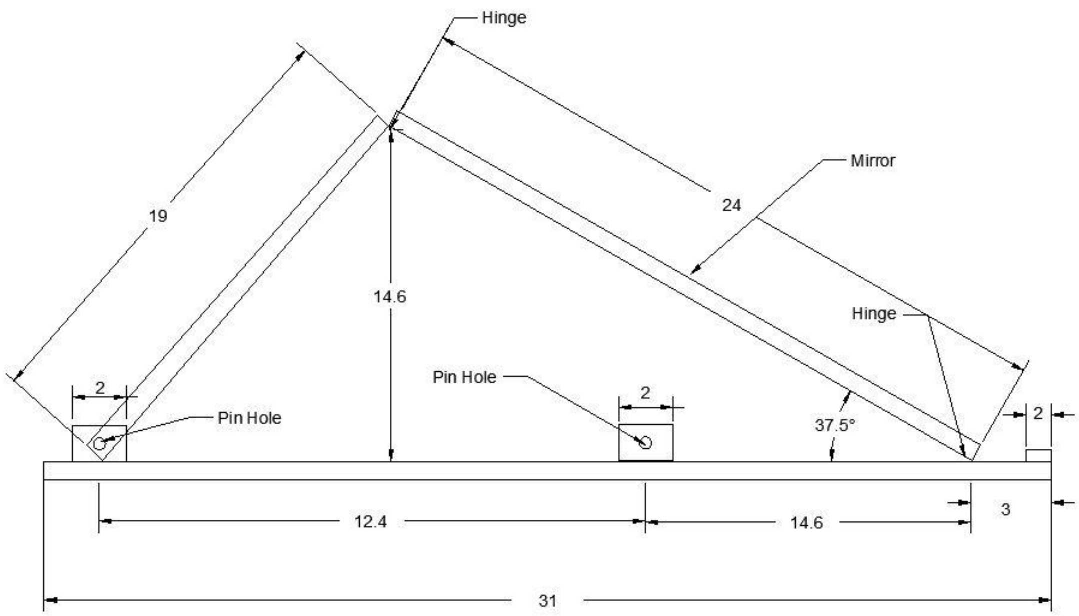

Figure 6-10. Drawing of Reflecting Mirror Adjusted at 37.5°

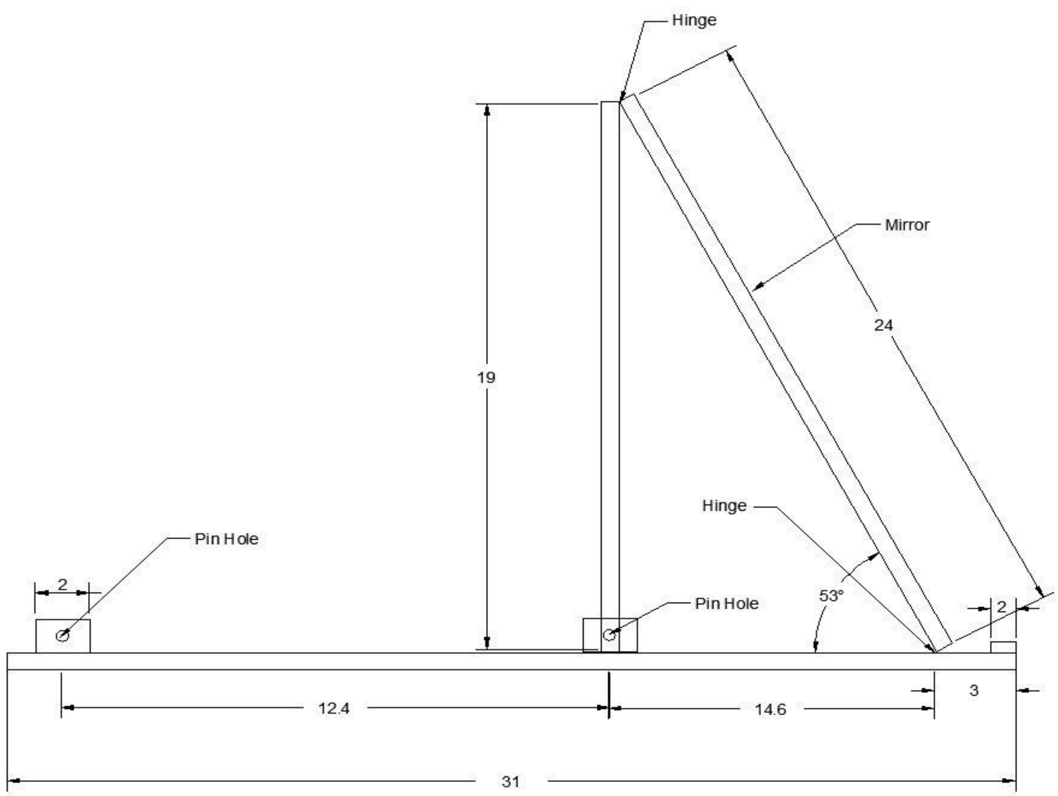

Figure 6-11. Drawing of Reflecting Mirror Adjusted at 53°

DC-DC Converter

A LM5088-1 evaluation board is being modified in this process. All the required components were soldered onto the board after removing the old components. After modifying the board, R_{RT} is changed to 24.9kΩ to achieve the desired frequency of 250kHz. The inductor is replaced with a 15μH, 2.6mΩ, and 1% tolerance to obtain I_{pp} being 26.67% of I_{out}. Other components such as the feedback resistor, sense resistor, ramp capacitor, and also the output capacitor were replaced as well. We then tested the board's functionality by conducting open circuit and full load tests.

Figure 6-12. LM5088-1

After all required components were replaced, female banana connectors were also installed for convinence testing purpose. Then the DC-DC converter was tested by using the Agilent E4356A Telecom DC Power Supply to meet the requirements.

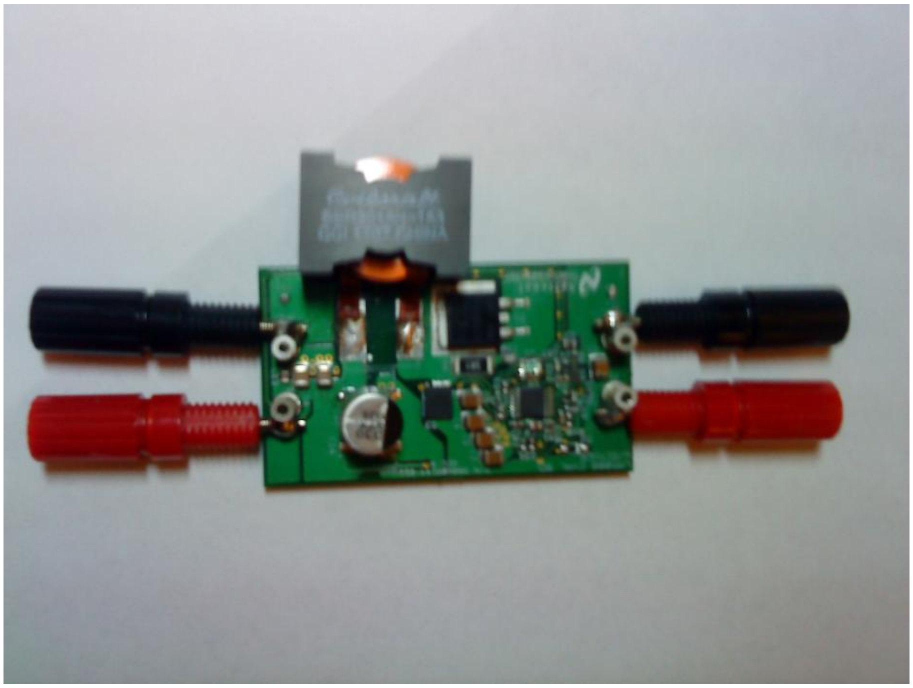

Figure 6-13. Re-designed LM5088-1

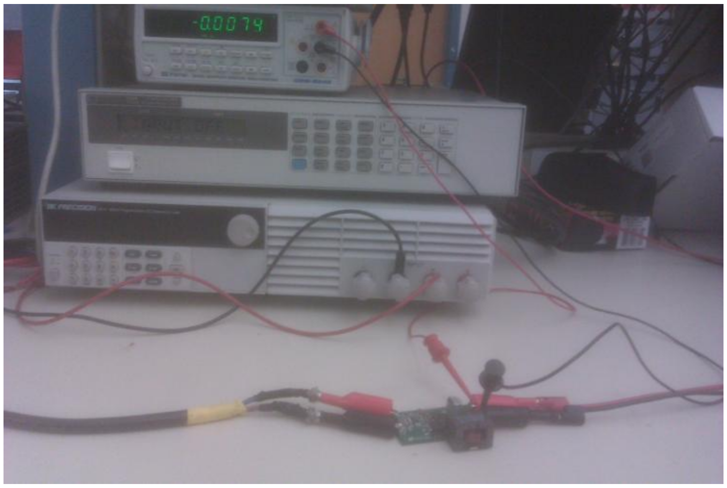

Figure 6-14. Agilent E4356A Telecom DC Power Supply

After constructing a fully developed DC-DC converter, we did open and full load testing to make sure it was still functionable. We would also compare the measured data of the Re-designed board with previous data to check if the modification would help increase the efficiency.

VII. Integration and Test Results

Integration

Before integrating both the solar panel and the DC-DC converter, we had to conduct testing for each component. After making sure how they performed individually, we integrated both components to conduct testing of their functionality. We connected the solar panel to the input of the converter and connected an electronic load to the output of the component. We also got measurements from the input and output of the converter. Furthermore, our project was able to operate and meet the requirements of our initial design.

Implementing Panel with Simulated Results

A stand with prescribed adjustable angles for the solar panel assuming it is located in San Luis Obispo, California. As shown in the figures below, the frame is implemented to be adjustable at 7°, 32° and 55°.

The data confirmed the simulated results; the optimum angle for spring time should be 32°, which is supported by comparing the actual data taken near the end of the spring season on a sunny day.

TABLE 7-1
Solar Panel Average Outputs with 55° Tilted Angle

% Load	Iout (A)	Vout (V)	Power (W)
10	0.79	34.43	27.1997
20	1.59	33.48	53.2332
30	2.39	32.5	77.675
40	3.19	30.4	96.976
50	3.99	21.6	86.184
60	4.37	0.288	1.25856
70	4.37	0.24	1.0488

TABLE 7-2
Solar Panel Average Outputs with 32° Tilted Angle

% Load	**Iout (A)**	**Vout (V)**	**Power (W)**
10	0.79	34.4	27.188
20	1.59	33.7	53.63
30	2.39	33.2	79.4
40	3.2	31.1	99.42
50	3.92	28.67	112.4
60	4.55	28.24	128.5
70	4.92	28.88	142.1

TABLE 7-3
Solar Panel Average Outputs with 7° Tilted Angle

% Load	**Iout (A)**	**Vout (V)**	**Power (W)**
10	0.79	34.4	27.176
20	1.59	33.7	53.583
30	2.39	33	78.87
40	3.19	32.1	102.399
50	4	31.1	124.4
60	4.8	27.4	131.52
70	5.6	27.1	151.76

As shown in data gathered in Tables 7-1 to 7-3, all angles have similar output power at low load conditions. However, as the load was increased, the panel tilted at 55° was not able to supply the increased power demands. Also, at 40% load, the output power of the 7° and 35° arrangement was significantly higher than that at 55°. Since the latter part of May approaches the summer season, the output power of the 7° tilted angle is slightly higher than that at 35°.

A. Intensity of the Radiation

The amount of power being generated by the solar cells increases as the intensity of light radiated on the cells increases, as shown in Figure 4-4. There are various methods of amplifying the sunlight intensity. Some are costly and result in increasing the temperature of the panel tremendously, which will decrease its lifespan. Therefore, the photovoltaic system in this project is implemented with reflecting mirrors to increase the intensity of the sunlight. The benefits of using this design are simple, low cost, low temperature induction, and highly efficient. The reflecting mirror design is placed at a tilted angle at the foot of the solar panel, as show in Figure 7-4 below.

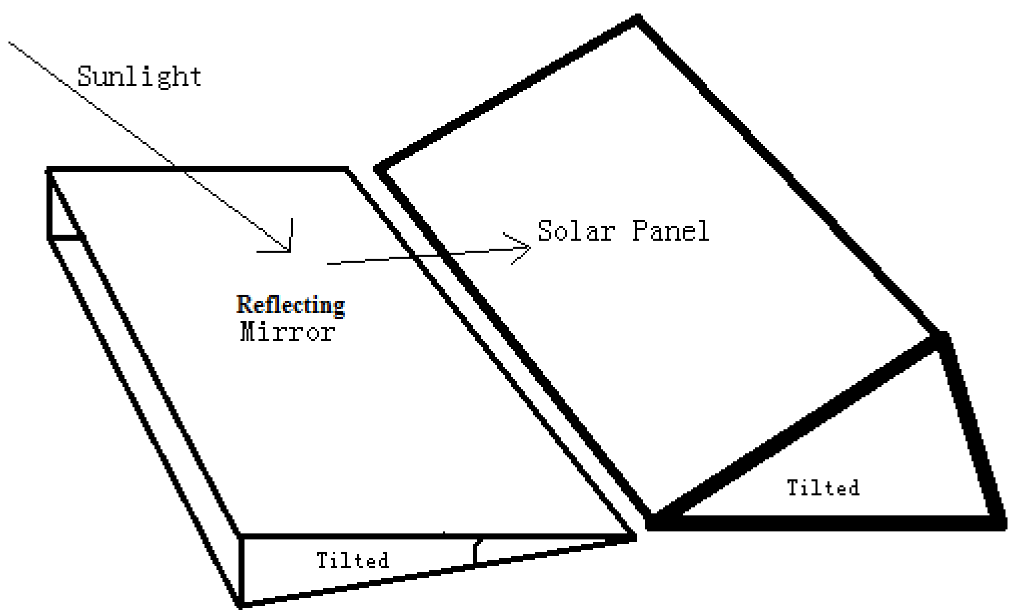

Figure 7-1. Maximizing Sunlight Intensity Method

A reflecting mirror with dimensions similar to the solar panel was selected and supported by an adjustable stand. The optimal angular orientations of the reflecting mirror were determined experimentally, as shown in Table 7-4 below.

TABLE 7-4
Optimal Reflecting Mirror Angular Orientations Average Output Data

Angle of Panel (Degrees)	Angle of Mirror (Degrees)	Average Output Current Without Mirror (A)	Average Output Current With Mirror (A)	% Increase
7	53	6.20	6.70	8.06
32	37.5	3.00	4.20	40.00
55	37.5	3.86	4.83	25.13

By analyzing the results from Table 7-4, a 10° reflecting mirror tilt I_{out} increased at a maximum of 8.06%. This was due to the harvested sunlight already at near maximum. Especially noteworthy, at 32° and 55° reflecting mirror tilts, I_{out} increased by 40% and 25.13%, respectively. For this reason, although adding another reflecting mirror has the potential to increase power, increasing the number of reflecting mirrors give rise to a poor cost-benefit ratio with decreasing advantage. Therefore, including additional reflecting mirrors in the design was rejected.

B. DC-DC Converter Testing

Testing of the Evaluation Board of LM5088 from National Semiconductor yields results as shown in Table 7-5 and Figure 7-2:

TABLE 7-5
Testing of the LM5088 Evaluation Board

I load (%)	I out (A)	Vout (V)	Vin (V)	Iin (A)	Power Out (W)	Power In (W)	Efficiency	%
10	0.7	4.965	6	0.606	3.4755	3.636	0.956	95.59
20	1.4	4.965	6	1.215	6.951	7.290	0.953	95.35
30	2.1	4.964	6	1.837	10.4244	11.022	0.946	94.58
40	2.8	4.964	6	2.48	13.8992	14.88	0.934	93.41
50	3.5	4.964	6	1.566	17.374	16.217	0.933	93.34
60	4.2	4.964	6	1.675	20.8488	19.460	0.933	93.34
70	4.9	4.964	6	1.755	24.3236	22.701	0.933	93.33
80	5.6	4.964	6	1.771	27.7984	25.941	0.933	93.32
90	6.3	4.964	6	1.832	31.2732	29.184	0.933	93.32
100	7	4.963	6	1.831	34.741	32.417	0.933	93.31

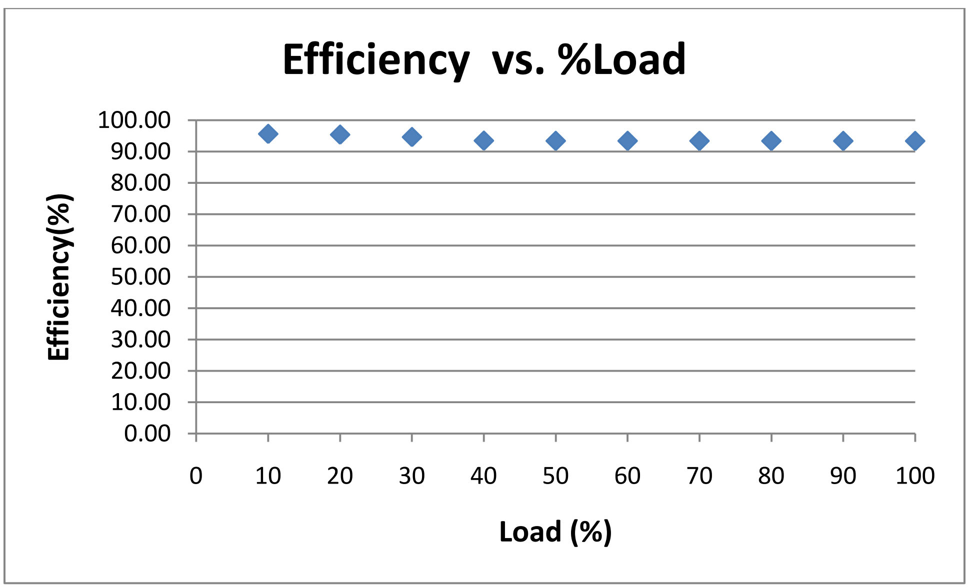

Figure 7-2. Efficiency Plot of LM5088 Evaluation Board.

Figure 7-2 shows the efficiency of the converter as the output load increases. Testing of the newly ordered evaluation board to ensure it is functioning properly. The converter

operated efficiently with loads up to 7A and maintained an output voltage of nearly 5V, which was the output voltage the evaluation board was designed for.

Testing of the Evaluation Board with feedback resistor = 270Ω:

TABLE 7-6
LM5088 Evaluation Board with Feedback Resistor Changed to 271Ω.

I load (%)	I out (A)	Vout (V)	Vin (V)	Iin (A)	Power Out (W)	Power In (W)	Efficiency	%
10	0.6	24.085	40	0.402	14.451	16.08	0.898694	89.8694
20	1.2	24.095	40	0.783	28.914	31.32	0.92318	92.31801
30	1.8	24.092	40	1.164	43.3656	46.56	0.931392	93.13918
40	2.4	24.091	40	1.545	57.8184	61.8	0.935573	93.55728
50	3	24.089	40	1.927	72.267	77.08	0.937558	93.75584
60	3.6	24.073	40	2.346	86.6628	93.84	0.923517	92.35166
70	4.2	24.076	40	2.72	101.1192	108.8	0.929404	92.94044
80	4.8	24.073	40	3.052	115.5504	122.08	0.946514	94.65138
90	5.4	24.081	40	3.394	130.0374	135.76	0.957848	95.78477
100	6	24.012	36.17	4.165	144.072	150.64805	0.956348	95.63483

From the table 7-6, the converter successfully maintained an output voltage of 24V by switching the feedback resistor to 271Ω.

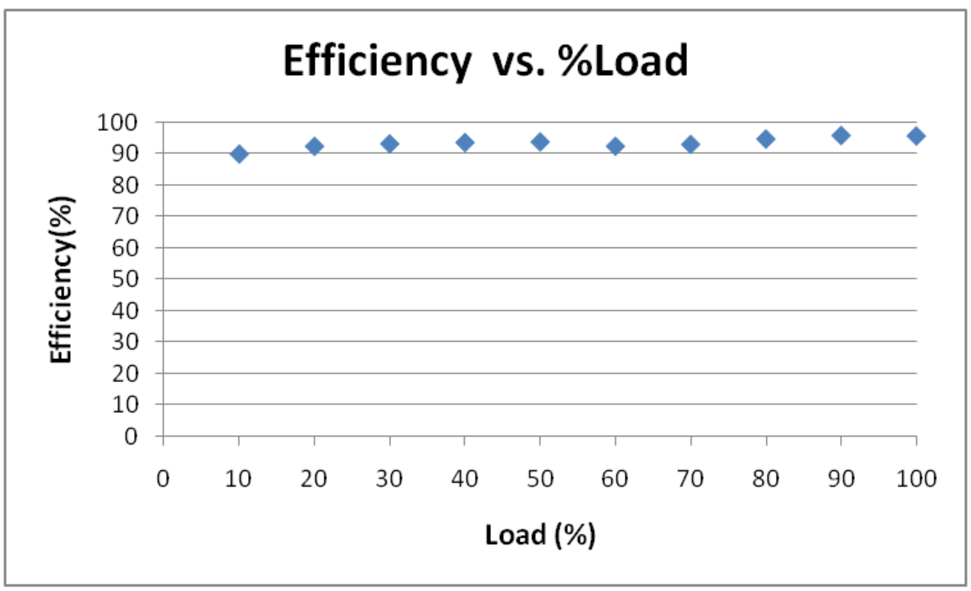

Figure 7-3. Efficiency of Converter with V_{out}=24V.

Figure 7-3 shows how the efficiency of the converter stays above 90%. This is expected from the converter since its bucking down the voltage and its dealing with high output. As it was explained before, non-synchronous buck converters tend to be as efficient as synchronous motors when their output are higher, like in this case 24V.

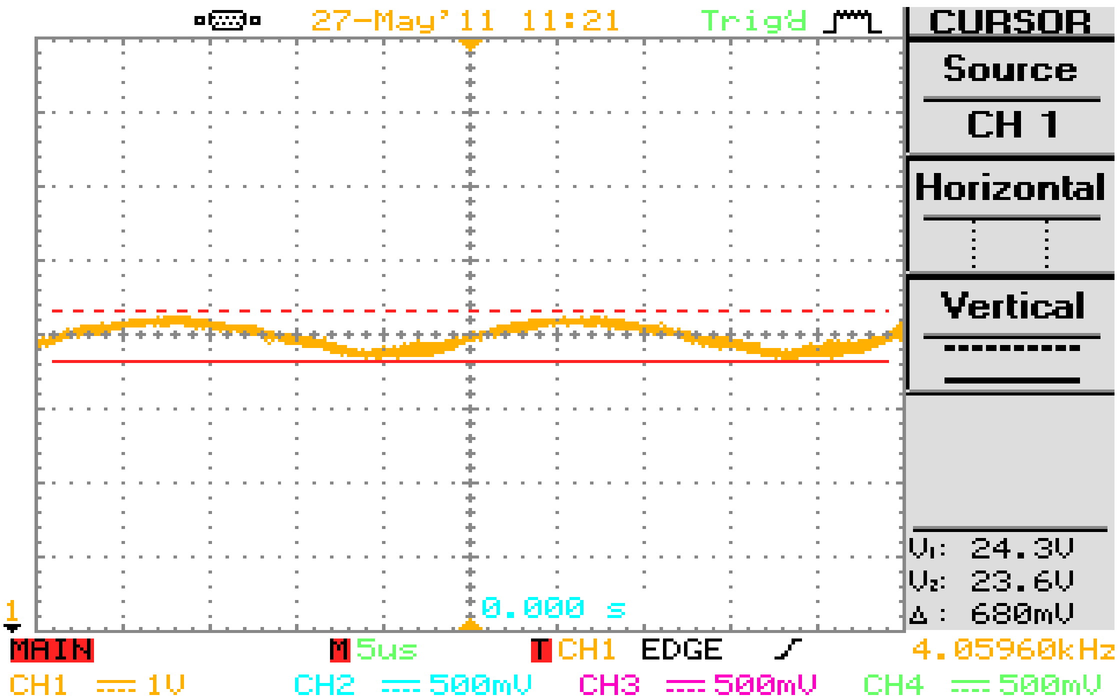

Figure 7-4. Full Load Voltage Output Ripple. The voltage peak to peak ripple is about 680mV.

TABLE 7-7
Converter Testing with Solar Panel Open Circuit Values

I load (%)	I out (A)	Vout (V)	Vin (V)	Iin (A)	Power Out (W)	Power In (W)	Efficiency	%
0	0	23.993	35.02	0.024	0	0.84048	0	0
10	0.81	24.107	35.02	0.613	19.52667	21.46726	0.909602343	90.96023
20	1.63	24.103	35.02	1.169	39.28789	40.93838	0.959683554	95.96836
30	2.42	24.101	35.02	1.725	58.32442	60.4095	0.965484237	96.54842
40	3.21	24.1	35.02	2.282	77.361	79.91564	0.968033291	96.80333
50	4.03	24.097	35.02	2.849	97.11091	99.77198	0.973328484	97.33285
60	4.82	24.095	35.02	3.416	116.1379	119.62832	0.970822795	97.08228
70	5.61	24.098	35.02	4.058	135.18978	142.11116	0.951296014	95.1296
80	6.43	24.097	35.02	4.635	154.94371	162.3177	0.954570635	95.45706
90	7.22	24.095	35.02	5.224	173.9659	182.94448	0.950921832	95.09218
100	8.03	24.096	35.02	5.812	193.49088	203.53624	0.950645841	95.06458

From Table 7-7, the converter is tested using Solar Panel Open Circuit Values, V_{in} = 35V and I_{in} = 7A. The converter is able to maintain an output of 24V. Under full load, the converter was able to input 203W and still output 193W, which is a success since there was a concern that the converter might not be able to handle 200W. Ultimately, the efficiency remained above 95%.

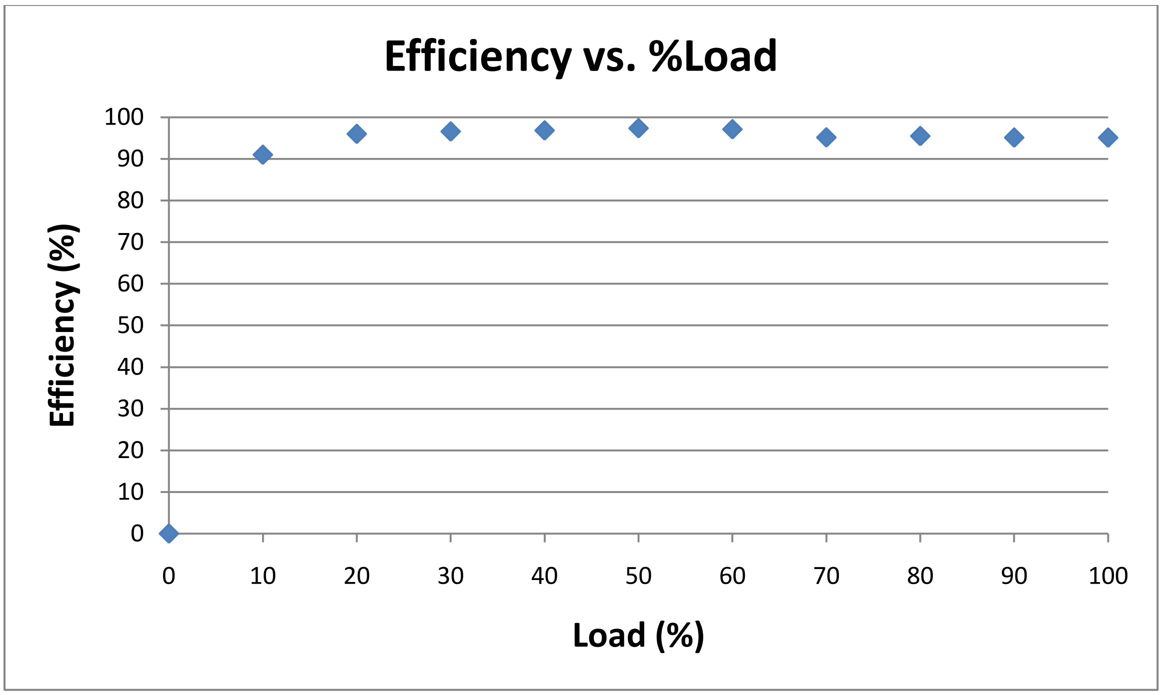

Figure 7-5. Efficiency Plot of Re-designed Converter

Figure 7-5 shows the efficiency of the buck converter as the load increases. The efficiency, being fairly high, nearly changed as an increase of output current was changing.

TABLE 7-8
Converter Testing with Solar Panel

	I load (%)	I out (A)	Vout (V)	Vin (V)	Iin (A)	Power Out (W)	Power In (W)	efficiency	%
	0	0	22.84	28.89	0.013	0	0.37557	0	0
	10	0.81	24.093	28.89	0.73	19.51533	21.0897	0.925348867	92.53489
	20	1.63	24.101	28.89	1.415	39.28463	40.87935	0.960989595	96.09896
	30	2.42	24.097	28.89	2.089	58.31474	60.35121	0.966256352	96.62564
	40	3.21	24.094	28.89	2.774	77.34174	80.14086	0.965072499	96.50725
	50	4.03	24.09	28.89	3.448	97.0827	99.61272	0.974601436	97.46014
	60	4.82	24.088	28.89	4.143	116.10416	119.69127	0.970030312	97.00303
	70	5.61	24.085	28.89	4.828	135.11685	139.48092	0.968712065	96.87121
	76	6	24.084	28.89	5.1496	144.504	148.77	0.9713	97.13
With Reflecting Mirror	80	6.43	24.083	28.89	5.513	154.85369	159.27057	0.972268072	97.22681

From Table 7-8, the converter was tested with the solar panel. The converter was unable to operate after exceeding 76% load because there was not enough sunlight for the solar panel to output enough power. However, with the help of the reflecting mirror, the panel was able to output enough power to supply up to 80% load.

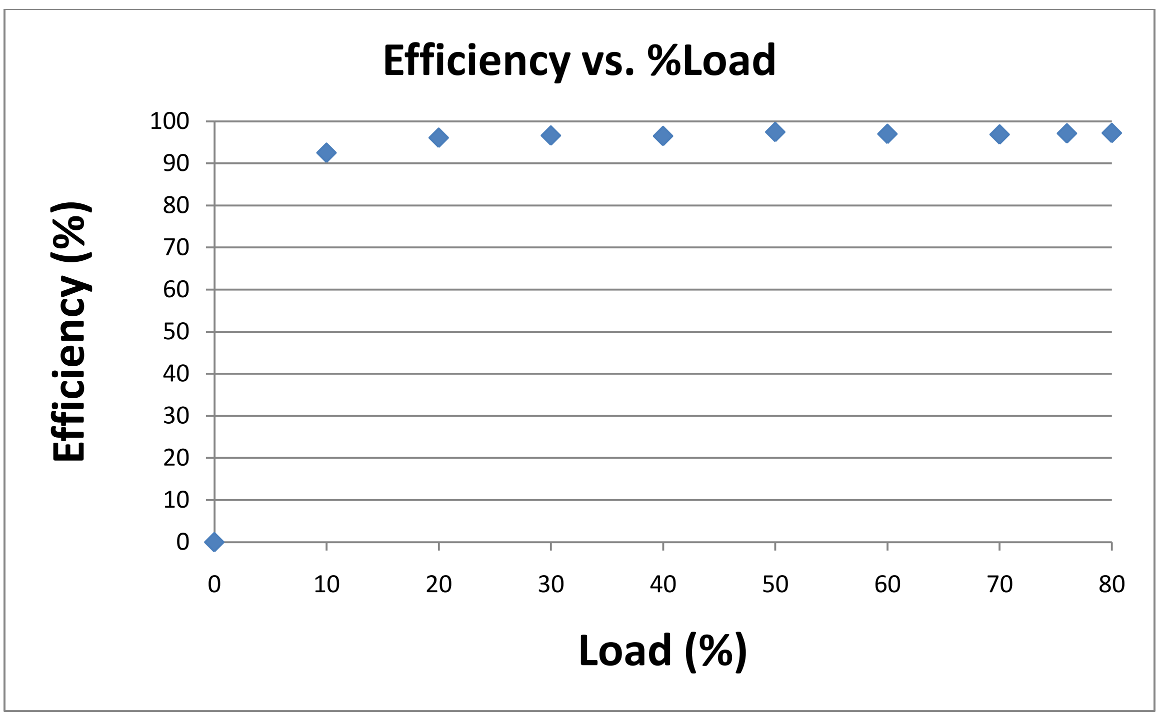

Figure 7-6. Efficiency Plot: Converter with Solar Panel

Figure 7-6 clearly shows how the efficiency stayed above 90% as the load was increasing. Even at max load the solar panel can support (80%) the converter and was able to be as efficient as it would be according to the datasheet. Having characteristic of high efficiency is what makes a converter a very useful component in the power world.

Calculations

Calculating the percent line regulation of the converter:

$$\%Line\ Regulation = \frac{V_{out(high\ input)} - V_{out(low\ input)}}{V_{out(nominal)}} * 100 \qquad (7\text{-}1)$$

$$\%Line\ Regulation = \frac{24.096V - 24.028V}{24V} * 100 = 0.075\%$$

Calculating the percent load regulation of the converter:

$$\%Load\ Regulation = \frac{V_{out(low\ load)} - V_{out(high-load)}}{V_{out(high\ load)}} * 100 \qquad (7\text{-}2)$$

$$\%Load\ Regulation = \frac{24.093 - 24.078V}{24.078V} * 100 = 0.06\%$$

Calculating efficiency in the system:

$$\eta = \frac{P_{out}}{P_{in}} = \frac{V_{out-avg} * I_{out-avg}}{V_{in-avg} * I_{in-avg}} \qquad (7\text{-}3)$$

The efficiency of the converter at full load:

$$\eta = \frac{P_{out}}{P_{in}} = \frac{154.84W}{159.57W} = 97.2\%$$

Peak to peak output voltage ripple at full load:

$$output\ voltage\ ripple\ \% = \frac{\Delta v_{RMS}}{V_{out}} \tag{7-4}$$

$$output\ voltage\ ripple\ \% = \frac{\Delta v_{RMS}}{V_{out}}\ x\ 100 = \frac{219.2mV}{24.078\ V}\ x\ 100 = 0.91\ \%$$

VIII. Conclusion

The simulated and measured results obtained for the DC-DC converter and solar panel design performed as expected. By adjusting the angles of the frame to account for the seasons, the solar panel may collect maximum sunlight throughout the year. The reflecting mirror was correspondingly adjusted to increase the output power of the solar panel by directing additional sunlight to the solar cells. Since solar cells are made of semiconductor material, the ambient temperature affects the performance of the solar cells. Airflow cooling the panel has the effect of increasing efficiency, according to the I-V characteristic curves of a solar panel.

The re-designed LM5088 Evaluation Board performed superbly, exceeding our expectations for the system. The DC-DC converter design achieved the following: 97% efficiency at full load (8.3A), 0.075% line regulation, 0.06% load regulation, and a ripple voltage of 0.91%. The combined photovoltaic panel and DC-DC buck regulator measured an output power is 194W, 3% short of our ideal goal of 200W. The design specifications for this project were achieved.

If the project development time were extended, more data could be collected to improve the optimum angle for each season. The solar panel stand and mirror stand would be constructed out of metal, increasing the durability.

Figure 8-1. Senior Project exhibition at California Polytechnic University of California, San Luis Obispo. Integration of Solar Panel Integrated with Reflecting Mirrors and DC-DC Converter.

IX. Bibliography

[1] Nathanial Gronewold. (2009, November 24). One-Quarter of World's Population Lacks Electricity. Avaliable: http://www.scientificamerican.com/article.cfm?id=electricity-gap-developing-countries-energy-wood-charcoal

[2] Peter Armstrong. (2006). Single-wire Earth Return. Available: http://www.stonepower.se/publications.htm

[3] Sheila Bocchine. (2007, October 15). Pros & Cons of Solar Power/Panels. Available: http://earth911.com/news/2007/10/15/pros-and-cons-of-solar-power/

[4] Windturbine. (2011, April 02). Wind Power From Wind Turbines. Available: http://windturbine.me/prosandcons.html

[5] V. Ryan. (2009). Advantages and Disadvantages of Hydropower. Available: http://www.technologystudent.com/energy1/hydr2.htm

[6] Lisa Zyga. (2007, June 1). 40% Efficiency Solar Cells to Be used for Solar Electricity. Available: http://www.physorg.com/news99904887.html

[7] European Photovoltaic Industry Association. (2009). Your Sun Your Enerygy. Available: http://www.epia.org/solar-pv/your-sun-your-energy.html

[8] Rich Nowakowski and Ning Tang. (2009). Efficiency of Synchronous versus Non-Synchronous Buck Converters. Available: http://focus.ti.com/lit/an/slyt358/slyt358.pdf

[9] National Semiconductor's WEBENCH®

[10] National Semiconductor LM5088-1 Evaluation Board Data Sheet

[11] Tamara Schmitz and Mike Wong. (2007). Choosing and Using Bypass Capacitors Available: http://www.intersil.com/data/an/an1325.pdf

[12] Solarpanelcenter.net. (2008). What Are Solar Panels. Available: http://www.solarpanelcenter.net/Types-of-Solar-Panels.php

[13] Pveducation.org. (2010). IV Curve. Available: http://www.pveducation.org/pvcdrom/solar-cell-operation/iv-curve

[14] Gary A. Becker. (2000, January). Astronomy Survival.
Available: http://www.astronomy.org/astronomy-survival/index.html

[15] Charles R. Landau. (2011, April 1). Optimum Orientation of Solar Panels.
Available: http://www.macslab.com/optsolar.html

[16] System Advisory Model (SAM) of National Renewable Energy Laboratory (NREL)

Appendix

A. Specifications

The converter:

1. Nominal Input Voltage = 26.4-36.2V
2. Nominal Output Voltage = 24V
3. Maximum Output Current = 8.33mA
4. Peak to peak output voltage ripple at full load of < 5%
5. Load regulation at nominal input with 10% to 90% load ≤ 2%
6. Line regulation at full load while input is changed from 26.4V to 36.2V ≤ 2%
7. Efficiency at full load ≥ 90%.

For the solar panel:

1. Nominal output Voc = 36.2V
2. Nominal output Isc = 7.67A
3. Nominal Maximum Power Output = 200W

B. Parts List and Costs

Solar panel used in the project

CS6P-200/205/210/215/220/225/230PE
e-Module

Electrical Data

		CS6P-200PE	CS6P-205PE	CS6P-210PE	CS6P-215PE	CS6P-220PE	CS6P-225PE	CS6P-230PE
Nominal Maximum Power at STC (Pmax)		200W	205W	210W	215W	220W	225W	230W
Optimum Operating Voltage (Vmp)		28.9V	28.9V	29.0V	29.0V	29.2V	29.4V	29.6V
Optimum Operating Current (Imp)		6.93A	7.09A	7.25A	7.40A	7.53A	7.65A	7.78A
Open Circuit Voltage (Voc)		36.2V	36.2V	36.4V	36.5V	36.6V	36.7V	36.8V
Short Circuit Current (Isc)		7.67A	7.78A	7.89A	8.01A	8.09A	8.19A	8.34A
Operating Temperature		-40℃~+85℃						
Maximum System Voltage		1000V (IEC) /600V (UL)						
Maximum Series Fuse Rating		15A						
Power Tolerance		+5W						
Temperature Coefficient	Pmax	-0.42%/℃						
	Voc	-0.35 %/℃						
	Isc	0.08 %/℃						
	NOCT	45℃						

Under Standard Test Conditions (STC) of irradiance of 1000W/m², spectrum AM 1.5 and cell temperature of 25℃

Mechanical Data

Cell Type	Poly-crystalline Solar Grade Silicon
Cell Arrangement	60 (6 x 10)
Dimensions	1638 x 982 x 40mm (64.5 x 38.7 x 1.57in)
Weight	20kg (44.1 lbs)
Front Cover	Tempered glass
Frame Material	Anodized aluminium alloy
Standard Packaging (Modules per Pallet)	20pcs

List of materials ordered for modifications of the LM5088 Demo Board

Part	Manufacturer	Part Number	Quantity	Price	Attribute 1	Attribute 1 Value	Attribute 2	Attribute 2 Value	Attribute 3	Attribute 3 Value
Cboot	Kemet	C0603C104K3RACTU	1	0.01	Cap	100nF	ESR	0Ohm	VDC	25V
Ccomp	Kemet	C0603C332K5RACTU	1	0.01	Cap	3.3nF	ESR	0Ohm	VDC	50V
Chf	MuRata	GRM1885C2A131JA01D	1	0.01	Cap	130pF	ESR	0Ohm	VDC	100V
Cin	CUSTOM	CUSTOM	1	0	Cap	16.023uF	ESR	500uOhm	VDC	53.333V
Cout	Nichicon	UUD1V151MNL1GS	2	0.23	Cap	150uF	ESR	0.17Ohm	VDC	35V
Cout1	Nippon Chemi-Con	EMVA100ADA330MD55G	1	0.07	Cap	33uF	ESR	0Ohm	VDC	10V
Cramp	MuRata	GRM1885C1H182JA01D	1	0.01	Cap	1.8nF	ESR	0Ohm	VDC	50V
Crst	Kemet	C0603C225K9PACTU	1	0.02	Cap	2.2uF	ESR	0Ohm	VDC	6.3V
Css	Kemet	C0603C103J5RACTU	1	0.01	Cap	10nF	ESR	0Ohm	VDC	50V
Cvcc	Kemet	C0603C225K9PACTU	1	0.02	Cap	2.2uF	ESR	0Ohm	VDC	6.3V
D1	Vishay-Semiconductor	50WQ10FNPBF	1	0.57	VFatIo	0.77V	Io	5.5A	VRRM	100V
L1	CUSTOM	CUSTOM	1	0	L	20.468uH	DCR	0.012Ohm	IDC	16.429A
M1	Infineon Technologies	BSC028N06LS3 G	1	0.99	VdsMax	60V	IdsMax	100A	Rdson45	4.8mOhm
Rcomp	Vishay-Dale	CRCW060364K9FKEA	1	0.01	Resistance	64.9KOhm	Tolerance	1%	Power	0.1W
Rfb1	Panasonic	ERJ-6ENF1961V	1	0.01	Resistance	1.96KOhm	Tolerance	1%	Power	0.125W
Rfb2	Susumu Co Ltd	RR1220P-363-D	1	0.01	Resistance	36KOhm	Tolerance	0.50%	Power	0.1W
Rramp	Vishay-Dale	CRCW060373K2FKEA	1	0.01	Resistance	73.2KOhm	Tolerance	1%	Power	0.1W
Rsns	Susumu Co Ltd	PRL1632-R006-F-T1	1	0.21	Resistance	6mOhm	Tolerance	1%	Power	1W
Rt	Vishay-Dale	CRCW060339K2FKEA	1	0.01	Resistance	39.2KOhm	Tolerance	1%	Power	0.1W
Ruv1	Panasonic	ERJ-6ENF2611V	1	0.01	Resistance	2.61KOhm	Tolerance	1%	Power	0.125W
Ruv2	Panasonic	ERJ-6ENF4992V	1	0.01	Resistance	49.9KOhm	Tolerance	1%	Power	0.125W
U1	National Semiconductor	LM5088MH-1	1	1.6						

C. Schedule – Time Estimates

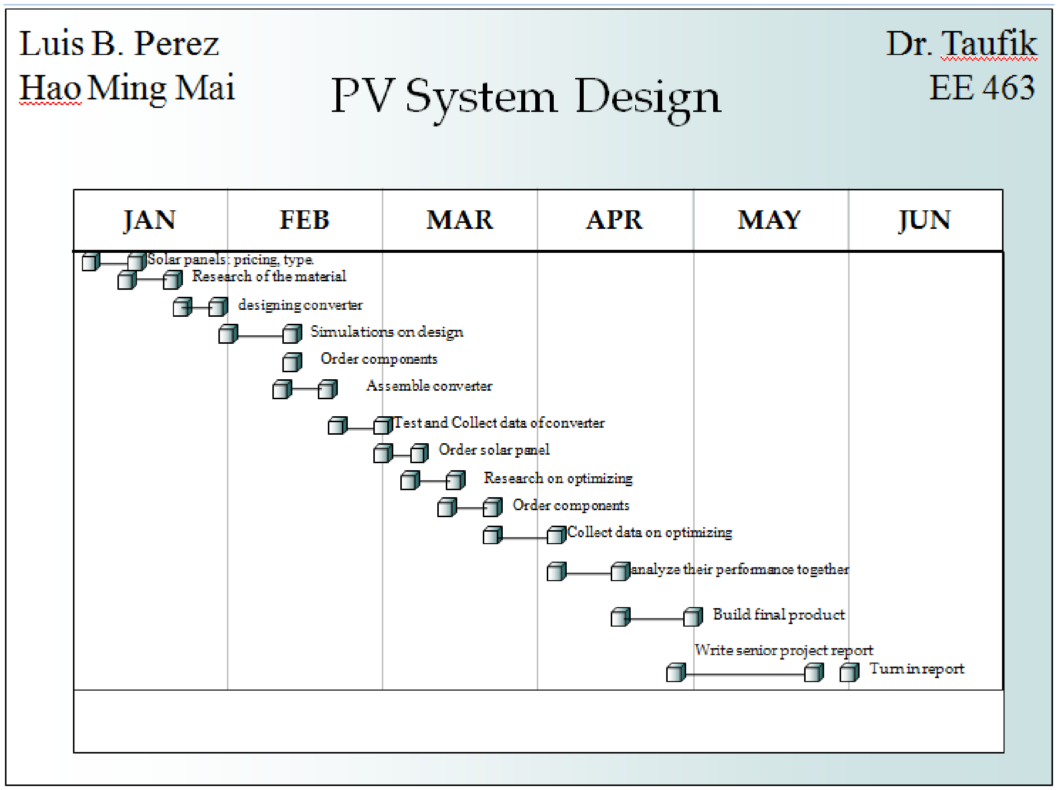

D. IC Location Diagram

LM5088 Demo Board circuit

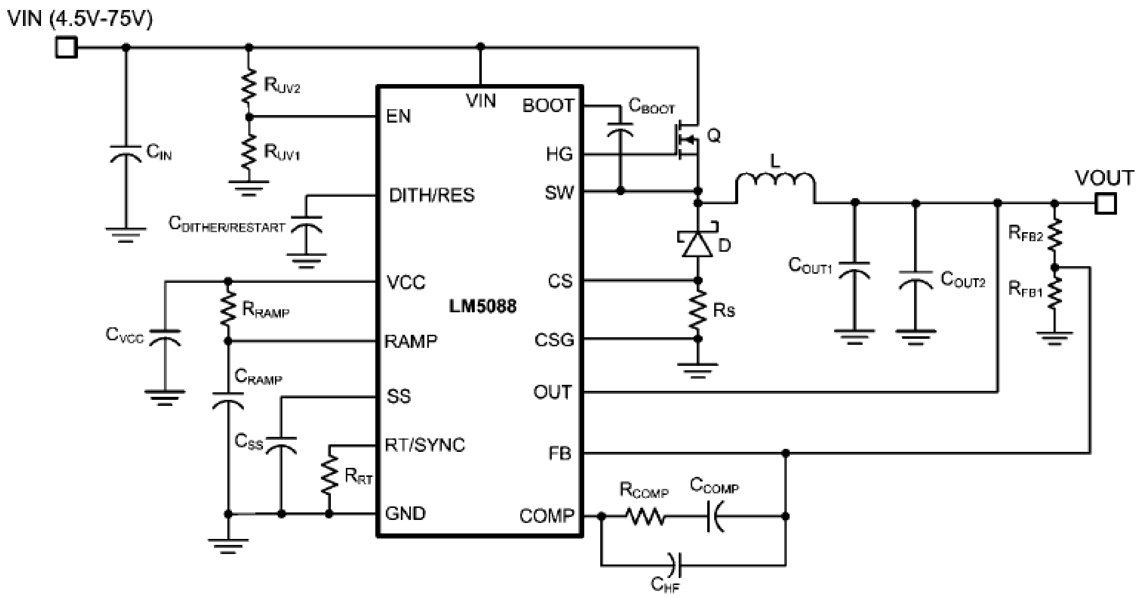

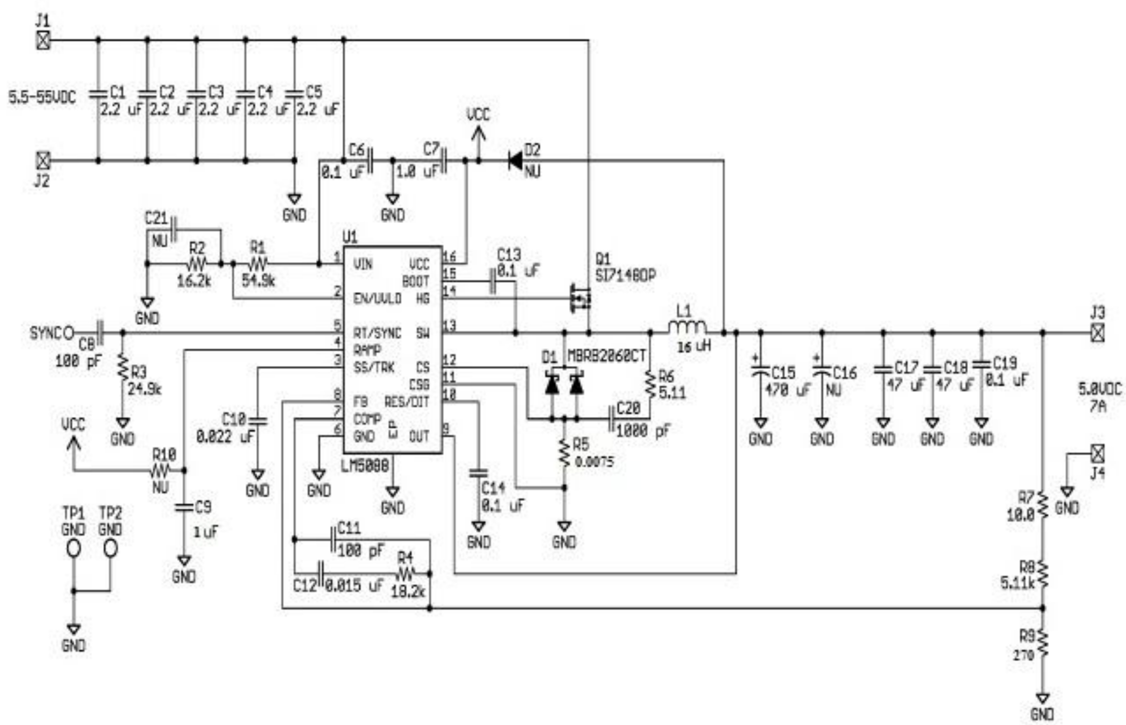

Material for making the stands:

Part	Quantity	Price (USD)
2x3-8 stud	4	7.48
2x2-8 wood	2	3.04
large strap hinges	4	15.88
small strap hinges	2	5.94
box of gold screws	1	6.47
eye bolt	4	1.96
13x49 mirror	2	11.96
wood glue	1	6.87

E. PC Board Layout and IC Locations